

Repository Istituzionale dei Prodotti della Ricerca del Politecnico di Bari

Refinement and Validation of the Simple Lateral Mechanism Analysis (SLaMA) Procedure for RC Frames

This is a post print of the following article

Original Citation:
Refinement and Validation of the Simple Lateral Mechanism Analysis (SLaMA) Procedure for RC Frames / Gentile, R., del Vecchio, C., Pampanin, S., Raffaele, D., Uva, G.. - In: JOURNAL OF EARTHQUAKE ENGINEERING. - ISSN 1363-2469. - ELETTRONICO. - 25:7(2021), pp. 1227-1255. [10.1080/13632469.2018.1560377]

Availability:
This version is available at http://hdl.handle.net/11589/176241 since: 2022-06-07

Published version
DOI:10.1080/13632469.2018.1560377

Publisher:

Terms of use:

(Article begins on next page)

17 November 2026

Refinement and Validation of the Simple Lateral Mechanism Analysis (SLaMA) Procedure for RC Frames

Roberto Gentile[a], Ciro del Vecchio[b], Stefano Pampanin[c], Domenico Raffaele[d], and Giuseppina Uva[d]

[a]Institute for Risk and Disaster Reduction, University College London, London, UK; [b]Department of Structures for Engineering and Architecture, University of Napoli Federico II, Napoli, Italy; [c]Department of Structural and Geotechnical Engineering, Sapienza University of Rome, Rome, Italy; [d]Department of Civil, Environmental, Landscape, Building Engineering and Chemistry, Polytechnic University of Bari, Bari, Italy

ABSTRACT

The 2017 New Zealand Society for Earthquake Engineering (NZSEE) guidelines for seismic assessment of buildings recommends using Simple Lateral Mechanism Analysis (SLaMA) before implementing numerical analyses. The method and the NZSEE guidelines have been enhanced from the 2006 version, resulting into an efficient procedure, balancing simplicity and accuracy.

This paper presents a numerical study, initiated as part of the development of the SLaMA-2017 method, to investigate the accuracy of the analytical approach via comparison with numerical 2D- pushover on 40 RC frames. SLaMA is effective in capturing the plastic mechanism of the frames, including global or soft-story mechanisms. Further-yet-simple refinements of the procedure are suggested.

1. Introduction

Several difficulties arise in the seismic assessment of existing buildings, as the lack of capacity design principles and adequate reinforcement details, among many other "deficiencies," strongly affect the structural response. Nowadays, it is widely recognized that nonlinear analyses, rather than linear approaches, are arguably the most reliable tool to characterize the lateral capacity of existing structures. Although they are available in user- friendly commercial software, their reliability and accuracy strongly depend on the ability of the numerical model to capture the probable failure mechanism, which in turns depends on the lateral capacity, both in terms of forces/moments and displacements/ rotations, of the main structural members and their mutual interaction. These aspects are difficult to capture and can lead to high uncertainties in the seismic response. Reliable yet simple assessment procedures are needed to identify potential structural weaknesses and their influence on the overall building capacity.

In the scientific literature, efforts were made in developing analytical nonlinear procedures such as [Borzi *et al*., 2008, Crowley *et al*., 2004, Cardone and Flora, 2017]. The spreadsheet – method that allows to define the nonlinear force– displacement capacity and the sequence of local and global mechanisms of a building system by using simple calculations. It was introduced for the first time in the 2006 version of the New Zealand Society of Earthquake Engineering, NZSEE, Guidelines for the "Assessment and Improvement of the Performance of buildings in earthquakes" [NZSEE, 2006], and significantly revamped in the 2017 version [NZSEE, 2017]. The procedure originates from a pioneering capacity design-based assessment procedure [Priestley and Calvi, 1991], later converted in a displacement-based assessment procedure by Priestley [1997]. This constitutes the basis of the procedure proposed in the NZSEE [2006] guide- lines, along with the capacity models for RC members reported in Priestley *et al*. [2007] and Pampanin et al. [2007b]. In the NZSEE [2017] guidelines "The Seismic Assessment of Existing Buildings", a significantly revised and enhanced version of the SLaMA procedure has been introduced as part of the Detailed Seismic Assessment. The application of SLaMA is required as an essential step before any other seismic numerical analysis is carried out.

A full example of the detailed implementation of the SLaMA procedure for a 3D,
torsion-prone RC case study building, damaged during the Canterbury Earthquake on February 22, 2011, along with a comparison with numerical nonlinear analyses (2D pushover, 3D time history) is reported in Del Vecchio *et al*. [2017a, 2018b]. Further research focused on the use of SLaMA as a tool to validate more sophisticated numerical models [Gentile *et al*., 2017a], or to rapidly develop fragility curves for RC frame buildings [Gentile *et al*., 2017b].

The significant effort in collecting, developing and simplifying the available procedures and the capacity models for existing RC structures resulted in the [NZSEE, 2017] version of the SLaMA. However, several issues still need to be addressed.

This paper presents the validation of the SLaMA procedure for RC bare frames, individuating the existing gaps and proposing refinements accordingly. In particular, a more refined estima- tion of the effective height for different plastic mechanisms is given, which also allows to estimate the displacement profile of the frame. Moreover, a new set of equations is given for Column-Sway (soft-story) mechanisms, which is valid for soft-story mechanisms located at any story of the frame.

An extensive parametric analysis over 40 case study frames with different geometry and mechanical properties is presented. The analytical capacity curves, the plastic mechanisms and the relevant parameters for the seismic assessment are calculated and compared with the results of refined numerical pushover analyses. Both the original

and the refined versions of SLaMA are considered. The comparison outlines the ability of SLaMA to capture the capacity curve and plastic mechanism of the frames (global or soft-story). The limitations of the procedure are discussed and suggestions for further researches are given. In particular, it is acknowledged that RC frames usually interact with infill walls. This may significantly affect the lateral response of the structural system resulting significant increase of the lateral stiffness, higher seismic forces and possible brittle failures both in the structural and nonstructural members [Magenes and Pampanin, 2004]. Although such interaction is of great interest, it is outside the scope of this paper and further research is needed.

2. Overview of the SLaMA 2017 Procedure for RC Frames and Proposed Refinements

SLaMA is an analytical procedure that allows to assess the nonlinear capacity (force vs deformation) and the plastic mechanism of a structural system starting from the capacity of the primary structural members/systems [NZSEE, 2017]. Since it relies on basic principles (i.e. equilibrium and compatibility), SLaMA is referred to as a "by hand analytical pushover analysis" since all the calculations can be easily implemented in a spreadsheet. Given the "deficiencies" of existing buildings (e.g. lack of capacity design, inadequate joint panel reinforcement), there is a need for practical implementation tools to test the reliability of numerical models in predicting the plastic mechanism. SLaMA aims to address this need, together with supporting the selection of retrofit strategies/ techniques at earlier stages of the assessment process.

With reference to RC bare frames, a proposed flowchart of the SLaMA procedure is depicted in Fig. 1. The NZSEE [2017] SLaMA procedure is therefore described on a step- by-step basis, highlighting the proposed refinements.

The first step of the SLaMA is the characterization of the lateral response of the main structural members (i.e. beams, columns, beam-column joints) composing the frame. The interaction between the members in the beam-column joint subassemblies is studied using the hierarchy of strength principle [Pampanin et al., 2007b]. Once the failure mode of the subassembly is detected, its strength and deformation capacity are assessed using equili- brium considerations. It is proposed to use the results of the hierarchy of strength for all the subassemblies to identify the probable plastic mechanism of the frame. Sets of equations are given to calculate the capacity curve for three recurrent plastic mechanisms. A "Column-Sway" (soft-story), with plastic hinges at the top and the bottom of all the columns of a given story, a "Beam-Sway," global mechanism characterized by plastic hinges at the end of all the beams, and a "Mixed-Sway," in which a combination of beam, column and/or joint failures can be triggered.

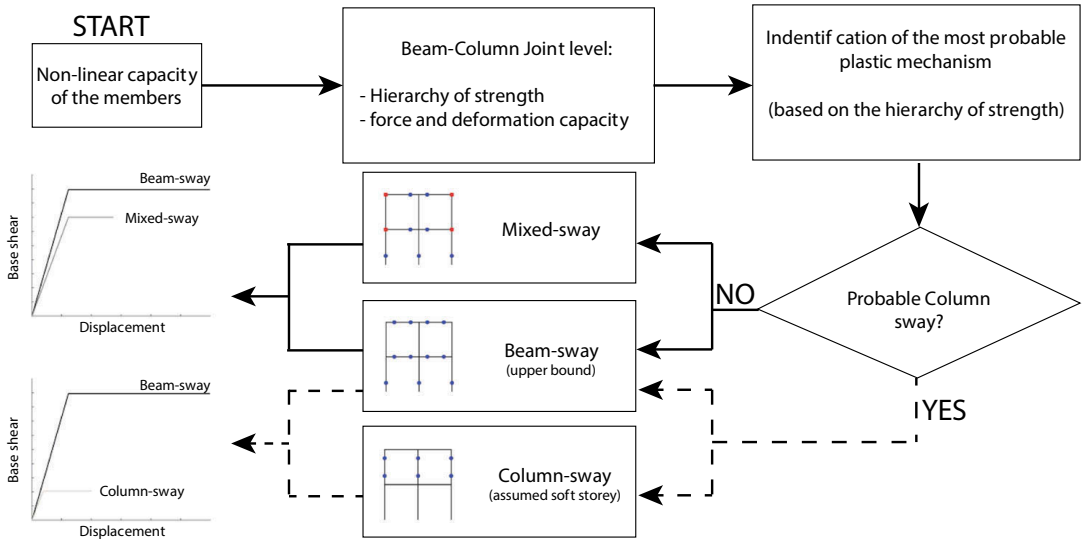


Figure 1. Proposed flowchart for the refined SLaMA procedure.

If a Column-Sway is likely to develop (which is likely to be the lower bound of the capacity for pre-1970s buildings designed without proper capacity design considerations), the related capacity curve is calculated. Otherwise, the Mixed-Sway case is more likely to develop, and the related capacity curve is calculated. In both cases, a "Beam-Sway" capacity curve is also calculated. This gives a measure of the upper bound of the force/ displacement capacity, since this refers to the highest capacity a frame can develop. This might be the case of well-designed RC frames in compliance with capacity design principles or the target for an optimal retrofit intervention for the frame.

For the described SLaMA procedure, the following assumptions hold:

- first vibration mode response dominates the behavior of the Lateral Resisting System;
- floor slabs are rigid in plane, acting as a diaphragm. This is a reasonable assumption for cast in-situ flat slabs;
- the columns are fully fixed at the base;
- for global mechanisms (Beam-Sway or Mixed-Sway), it is assumed that all the beam- column joint subassemblies in the frame can exploit their maximum strength capa- city, (determined according to the hierarchy of strength);
- the frame strength is calculated based on the expected plastic mechanism;
- any hardening of the structural members is conservatively neglected in the calcula- tion of the global base shear, hence the global base shear at yielding and ultimate are equal. Conversely, member hardening is considered in the calculation of the hierarchy of strength calculation, since it may greatly affect such a prediction.

2.1. *Members Capacity Curves*

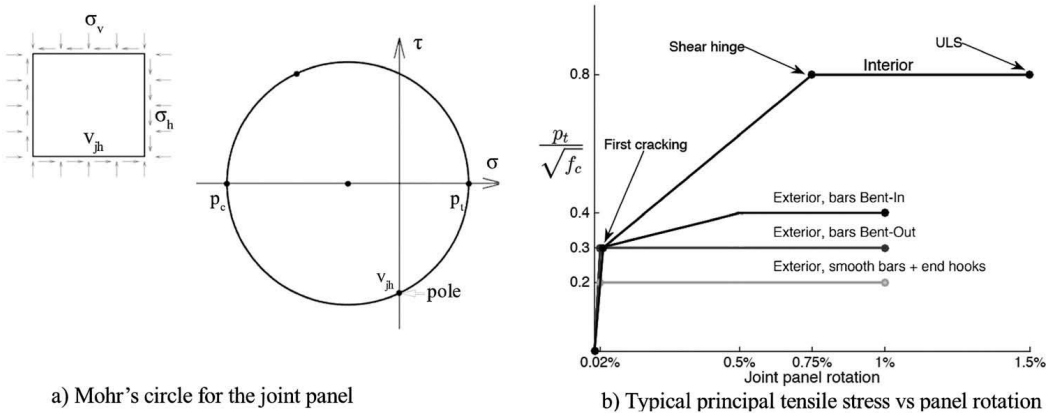
The lateral response and the most probable failure mechanism of the structural members (i.e. beams, column and beam-column joints) should be assessed using reliable capacity models. In this section, the capacity models suggested in [NZSEE, 2017] are summarized while a detailed description and the step-by-step calculations for existing RC members are reported in Gentile [2017] and Del Vecchio *et al*. [2017a].

The flexural capacity of the RC members can be derived using reliable numerical or analytical procedures and including the effect of the axial load. Then, the flange effect [Quintana-Gallo, 2014, NZSEE, 2017], lap splice failure [Priestley *et al*., 1996], shear failure [Kowalsky and Priestley, 2000, Elwood and Moehle, 2005, Del Vecchio *et al*., 2017c], bar buckling [Berry and Eberhard, 2005] should be considered, as they can significantly modify the lateral response of the members (Table 1).

Table 1. Capacity models for the characterization of the members.

Bar buckling drift [Berry and Eberhard, 2005]	$\theta_{bb} = \frac{3.25\left(1+k_{e_bb}\,\rho_{eff}\frac{d_b}{D}\right)\left(1-\frac{P}{A_g f_c'}\right)\left(1+\frac{L_c}{10D}\right)}{100}$
Shear strength for beams and columns [Kowalsky and Priestley, 2000]	$V_p = 0.85\left(\alpha\beta\gamma\sqrt{f_c'}b_w d + Ptana + \frac{A_v f_{yh} d}{s}\right)$
Ultimate displacement for flexure-shear failure [Elwood and Moehle, 2005]	$\Delta_s = L_v\left(0.03 + 4\rho_s - 0.024\frac{v}{\sqrt[3]{f_c'}} - 0.025\frac{P}{A_g f_c'}\right) \geq 0.01 L_v$

where: ρ_s ; f_{yh}: volumetric ratio and yield stress of the transverse reinforcement; $k_{e\ bb}$: transverse reinforcement coefficient; ρ_{eff}: effective confinement ratio; d_b: average diameter of longitudinal reinforcement; D: section effective depth; P: member axial load; A_g: gross section area; $f_{\ 0}$: unconfined concrete strength; L_v: shear span; α; β; γ: aspect ratio, dowel effect and shear strength degradation factors; b_w: width of section web; d: effective depth of section; s: stirrup spacing; v: shear stress ratio.



a) Mohr's circle for the joint panel

b) Typical principal tensile stress vs panel rotation

Figure 2. Typical joint capacity curves for different detailing.

The principal stress approach, combining joint shear and gravity load, is adopted to calculate the horizontal joint shear strength (V_{jh}). Figure 2 shows the experimentally validated limits for the principal tensile/compressive stress p_t; p_c used for the calibration of the joints [Priestley, 1997, Pampanin *et al*., 2003, NZSEE, 2017]. It is worth mentioning that the selected values for the joint ultimate drift (1% for exterior, 1.5% for interior) are equal to the drift for which the onset of strength degradation was experimentally observed [Pampanin *et al*., 2003, Del Vecchio *et al*., 2018a]. Therefore, joint strength degradation has been neglected in this study resulting in conservative estimations of the ultimate displacement capacity of the frame."

2.2. *Strength and Deformation Capacity of Beam-Column Joint Subassemblies*

The global performance of a frame structure can be assessed by characterizing the performance of the beam-

column joint subassemblies, that is, the portion of the frame enclosed by the contra-flexure points of beams and columns (assumed at mid span). If the failure mechanism of the weakest member in the subassembly allows hardening, and hence further increase of the lateral force, another mechanism may activate. For example, the first shear cracking of the joint panel allows the increase in the external force until, for instance, a beam hinge develops (see Fig. 3c).

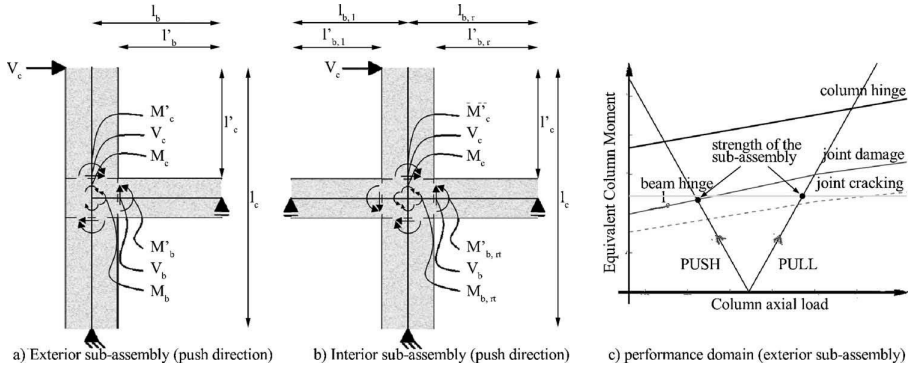


Figure 3. Subassemblies: rotational equilibrium about the joint centroid.

As suggested in Calvi *et al*. [2002] and Pampanin et al. [2007b], to compare different members and failure modes the Equivalent Column Moment (*ECM*) is used. This is the moment in the column, calculated at the joint interface, corresponding to a given member failure mechanism in the subassembly. By means of equilibrium conditions at subassembly level (Fig. 3), this is calculated for each member failure mechanism and plotted in an Equivalent Column Moment-axial load performance domain (Fig. 3c, related to an exterior subassembly). For instance, the Equivalent Column Moment corresponding to the yield moment of the beam (which does not vary with the column axial load) corresponds to a horizontal line in the performance domain.

The seismic demand on the subassembly due to the lateral sway of the frame is defined in the M-N domain by two straight lines anchored in the point corresponding to zero- moment and gravity axial load. Considering both directions of the seismic action, the demand appears as a V-shaped curve. The slope of the lines corresponds to the ratio of the seismic moment to seismic axial load on the column (M_E=N_E). Details on this calculation are given in Gentile [2017] and Del Vecchio *et al*. [2017a].

The formulations for the Equivalent Column Moment are summarized in Table 2 (see also Fig. 3). Some modifications are made with respect to [NZSEE, 2017] to account for the different lengths for the left and right beams in interior sub-assemblies. Besides, this refinement allows for the accurate determination of the hierarchy of strength if the yielding moment of left and right beams varies significantly. It is worth mentioning that for interior and exterior roof subassemblies, the same formulations can be used, provided that the net column length (l_c^0) is divided by two. The strength of a sub-assembly ($M_{c\omega 0}$; Where symbol´ indicates that this is computed at the column/joint interface) depends on the first mechanism in the hierarchy of strength that does not allow any further increase in the external forces. With reference to the performance domain in Fig. 3c, in the "push" direction (corresponding to a decreasing axial load on the column) the first cracking of the joint is likely to develop first. If deformed beam bars are bent into the joint panel, the shear force can further increase (see Fig. 2) and the next mechanism (joint failure) can be triggered. Therefore, in the "push" direction, the strength of the sub-assembly is characterized by the ECM corresponding to the joint failure. In the "pull" direction (corresponding to an increasing axial load on the column), the beam yields after the joint first cracking. Beam hardening allows for further increases in the external forces, but this is not sufficient to activate the next mechanism. Therefore, the strength of the subassembly is related to the ECM correspond- ing to the beam flexural yielding.

Once the ECM corresponding to the strength of the subassembly is calculated ($M_{c\omega 0}$), the related Equivalent Beam Moment ($M_{b\omega}$) can be computed with Eq. 1 imposing rotational equilibrium about the joint centroid (see Fig. 3) and assuming that the beam moment is equally distributed in the top and bottom columns. n_{cols} and n_{beams} represent the number of columns and beams framing in a joint.

$$M_b^* = \frac{n_{cols} M_c^*}{n_{beams}}, \text{where :} \quad (1)$$

$$M_c^* = \frac{l_c}{l_c'} M_c^{*'} \quad (2)$$

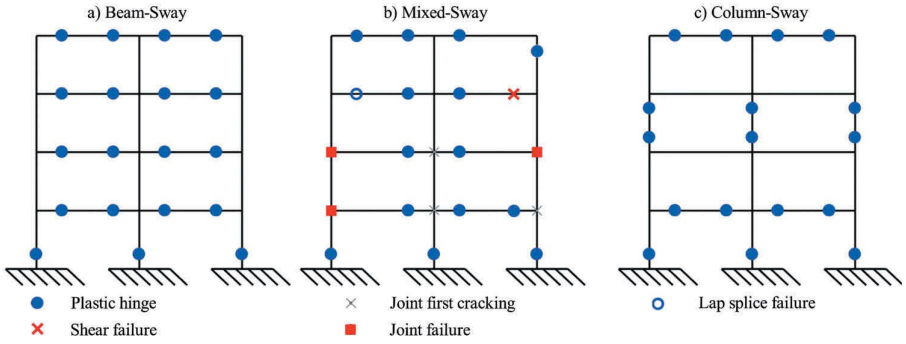


Figure 4. Examples of hierarchy of strength resumes for 2-bays, 4-stories frames (push direction, external forces from pointing right).

Many experimental tests on subassemblies [e.g. Pampanin *et al*., 2002, Calvi *et al*., 2002, Del Vecchio *et al*., 2018] demonstrated that the beams, the columns and the joint panel contribute to the total drift. However, most of the inelastic deformation is concentrated in the weakest member, whose drift is used to determine the drift capacity of the subassem- bly. For this example, the yield ($\theta_{sub\ y}$) and ultimate ($\theta_{sub\ u}$) drifts of the subassembly, in the "push" direction, are equal to the joint panel drift limits corresponding to the joint cracking and the joint shear failure, respectively. In the "pull" direction, the beam yielding and ultimate drift govern the deformation of the subassembly.

2.3. *Plastic Mechanism and Definition of the Capacity Curve*

The probable plastic mechanism of the frame is assessed based on the hierarchy of strength of all the subassemblies that compose the frame. Figure 4a indicates a "Beam-Sway" mechanism, in which plastic hinges develop in all the beams at all the stories, along with the flexural yielding of the base columns. If any joint shear failures, column plastic hinges (except from the base), shear failures in beams and/or columns or lap-splice failures is predicted, the plastic mechanism is called "Mixed-Sway" (Fig. 4b). Finally, if the hierarchy of strength leads to a soft-story behavior, for which Fig. 4c is an example, the mechanism is a "Column-Sway." For asymmetric frames, either in geometry or in the strength of the members, the same process should be repeated using the hierarchy of strength in the "pull" direction, checking for major changes in the result, and possibly calculating two different capacity curves.

As a general approach, the bilinear representation of the frame capacity curve is calculated using global equilibrium and by considering the member(s) causing yielding and the ultimate limit state. An approximate displacement shape is assumed. Different formulations to derive the frame base shear are available for each plastic mechanism type (i.e. Beam-Sway, Mixed-Sway and Column-Sway).

2.3.1. *Beam-Sway Mechanism*

According to the NZSEE [2017] procedure, unchanged herein, the overturning moment

$$OTM = \sum F_i H_i$$

where H_i is the height of the i^{th} story from the foundations) resisted by the structure at Ultimate Limit State (ULS) can be calculated with Eq. 3, in which j is the considered joint and i indicates the story, M_{cy} is the column yielding moment, $M_{by;l}$ and $M_{by;r}$ are the left and right beam yielding moments and L^{ext} is the length of the external bay. For regular frames with the beams at the same story that have the same moment capacity, only the moments on the external beams are used. An extended procedure valid for irregular frames can be found in [Priestley *et al*., 2007]. The base shear capacity of the frame is obtained dividing the OTM by the effective height of the frame in a Beam-Sway configuration (H^{BS}, Eq. 4). The effective height is calculated with Eq. 5, using the ultimate displacement profile Δ^u (calculated as shown below in this section). P-Delta effects might be considered subtracting the second order overturning moment ($OTM^{P\Delta}$) to the first order capacity. For the ultimate point of the capacity curve, Eq. 6 can be used, where P_i is the sum of the vertical gravity loads at story i. A linear interpolation should be considered between the origin and the ultimate condition. It is worth mentioning that this aspect is outside the scope of this paper and needs further validation.

$$OTM^{BS} = \sum_j M_{cy\,j} + \sum_i \frac{M_{by,l\,i} + M_{by,\,r\,i}}{L_{bay}^{ext}} L \tag{3}$$

$$V_B^{BS} = \frac{OTM^{BS}}{H_{eff}^{BS}} \tag{4}$$

$$H_{eff}^{BS} = \frac{\sum_i m_i \Delta_i^u H_i}{\sum_i m_i \Delta_i^u} \tag{5}$$

$$OTM^{P\Delta} = \sum_i P_i \Delta_i^u \tag{6}$$

Each subassembly is characterized by the yield ($\theta_{sub\ y}$) and ultimate ($\theta_{sub\ u}$) drift capacity. For a Beam-Sway mechanism these are equal to the beam yield and ultimate drift, respectively. According to the SLaMA procedure proposed in the NZSEE [2017], the yielding and ultimate displacement of the frame at the effective height can be computed as the product of the effective height and the minimum yielding or ultimate drift of the beams, respectively. Although this is a very simple method, this is a clear approximation, since it does not capture the dependency of the effective height on the number of stories. Indeed, a fixed value equal two-thirds of the total height is suggested in NZSEE [2017].

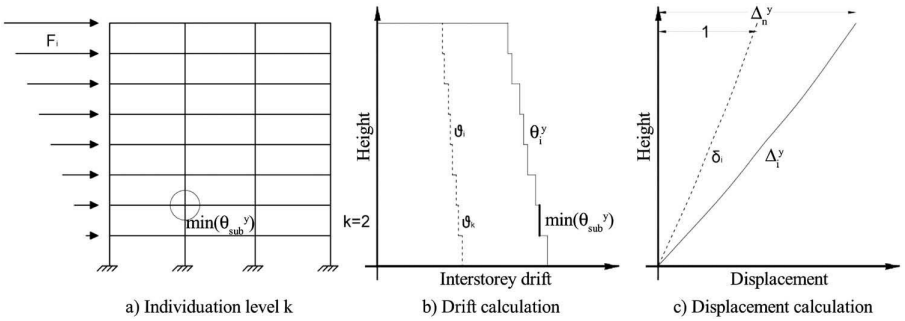


Figure 5. Calculation of the displacement profile at the yielding of the frame.

In the refined formulation proposed in this work, it is assumed that the displacement shape of the frame (δ_i) is governed by Eq. 7, proposed by Priestley *et al*. [2007], in which H_n is the total height. This results in a unitary displacement at the top (dashed line in Fig. 5c). The original formula by Priestley *et al*. [2007] assumes a linear displacement shape for frames with four stories or less and a nonlinear shape otherwise. Based on the parametric analysis in this work, it is suggested to reduce this threshold to 2, for applications within the SLaMA framework. The related drift shape can be calculated as

$$\vartheta = (\delta_i - \delta_{i-1})/(H_i - H_{i-1}),$$

corresponding to the dashed line in Fig. 5b. The adjacent story below the subassembly with the minimum yielding ultimate drift is named level *k* (highlighted with a circle in Fig. 5a). If two or more subassemblies have the same yield or ultimate drift, level *k* is the lowest. It may happen that level *k* for the ULS is not equal to level *k* for the yielding. The displacement profile (continuous line in Fig. 5c) at yielding (Δ^y) or ULS (Δ^u) can be computed by scaling the displacement shape (δ_i) by the factor

$$\min\left(\theta_{sub\ y/u}\right)/\vartheta_k,$$

This procedure is graphically shown in Fig. 5.

It is worth mentioning that the calculation of the frame yielding and ULS based on the minimum drift capacity of the subassemblies is simple but approximate, since the evolution of the internal actions over the frame is not accounted for. Finally, the displacement (at yielding and ultimate) at the effective height is calculated with Eq. 8, as proposed in Priestley *et al*. [2007].

$$\delta_i = \begin{cases} \frac{H_i}{H_n} \ for\ n \le 2 \\ \frac{4}{3}\left(\frac{H_i}{H_n}\right)\left(1 - \frac{H_i}{4H_n}\right) \ for\ n > 2 \end{cases} \tag{7}$$

$$\Delta^{y/u}\left(H_{eff}^{BS}\right) = \frac{\sum_i m_i \Delta_i^{y/u^2}}{\sum_i m_i \Delta_i} \tag{8}$$

Typically, the Beam-Sway mechanism is not likely to characterize the response of existing RC frames. However,

this capacity curve is the upper bound of the frame lateral capacity and it can provide useful information to design a proper retrofit solution.

2.3.2. *Mixed-Sway Mechanism*

The procedure for the calculation of the capacity curve related to a Mixed-Sway mechan- ism follows the steps explained for the Beam-Sway mechanism (Sec. 2.3.1). However, in this case the strength ($M_{b\omega}$ and deformation ($\theta_{sub\ y=u}$ capacity of the subassemblies are defined according to the refined hierarchy of strength (Sec. 2.2).

The displacement shape (δ_i) is calculated with Eq. 7 and then amplified by the ratio

$$\min\left(\theta_{sub\ y/u}\right)/\vartheta_k$$

where θ_k is the drift shape at level k (see Sec. 2.3.1).

The displacement at the effective height at yielding and ULS is calculated with Eq. 8. The overturning moment capacity (OTM^{MS}) is calculated with Eq. 9. It differs from Eq. 3 since the moment corresponding to the failure is considered for the columns ($M_{c\ j}$, i.e. flexure, shear or lap-splice) instead of the yielding. The Equivalent Beam Moment (Sec. 2.2) at the left ($M_{b\omega;l\ i}$) and right ($M_{b\omega;r\ i}$) ends of the external beams at all stories is used for this calculation. It is worth mentioning that, even for regular and symmetric frames, the Mixed-Sway OTM calculated using the left or right external beams can vary significantly. Hence, a mean value should be considered. After calculating the effective height with Eq. 5, the base shear capacity for the Mixed-Sway (V^{MS}) is calculated dividing the OTM capacity by the effective height.

$$OTM^{MS} = \sum_j M_{c\ j} + \sum_i \frac{M^*_{b,l\ i} + M^*_{b,r\ i}}{L^{ext}_{bay}} L \tag{9}$$

If the ULS of the frame is conditioned by a brittle failure mode of one or more members, for example, the shear failure in a column, yielding might be prevented. The ultimate displacement might be used to "trim" the first branch of the capacity curve and hence obtain the ultimate base shear. However, the initial stiffness of the capacity curve is based on the formation of a plastic mechanism (secant-to-yield stiffness) which is clearly inappropriate if a brittle behavior is expected. For this reason, the process of "trimming" the capacity curve yields a major error and it is therefore not suggested. An elastic force- based analysis, based on gross or cracked stiffness of the members, is suggested in such situation.

2.3.3. *Column-Sway Mechanism*

If the hierarchy of strength calculations for all the subassemblies indicate that a soft-story mechanism is likely to be triggered at level *s* (see Fig. 4c), a procedure alternative procedure to the one suggested in NZSEE [2017] is proposed to calculate the frame capacity curve. It is worth mentioning that the Column-Sway procedure proposed in NZSEE [2017] is theoretically valid only for soft-story mechanisms located at the first story. Moreover, a constant effective height (50% of the total height) is suggested, regard- less of the number of stories. The proposed procedure overcomes both issues. It can be employed independently of the location of the soft story and it allows the calculation of both the displacement profile and the effective height. It is worth mentioning that if two or more stories are "soft-story prone," based on the hierarchy of strength, different Column- Sway capacity curves are calculated. The capacity curve with the lowest base shear is considered as the most probable.

The peak shear strength of the soft-story level *s* ($V_{int\ s}$) depends on the capacity of the columns at that story (M_c, depending on their predicted failure mode). It can be calculated with Eq. 10, where *j* is the generic column at level *s*, $h_{int\ s}$ is the inter-story height of level s and h^{top} and h^{bot} are the average depths of the beams above and below story *s*.

$$V_{int\ s} = \frac{\sum_j M^{top}_{c\ j} + \sum_j M^{bot}_{c\ j}}{h_{int\ s} - \frac{h^{top}_b}{2} - \frac{h^{bot}_b}{2}} \tag{10}$$

If in a first approximation, it is assumed that the horizontal force profile is linear (Eq. 11), the shear demand for a unit base shear, V_B 1, can be calculated with Eq. 12. This assumption should be verified as shown below. As shown in Fig. 6, the base shear strength of the frame can be estimated by scaling the shear demand at level *s* related to the unit base shear ($V_s^{\delta 1 p}$) matching the shear capacity at that story ($V_{int\ s}$, see Eq. 13).

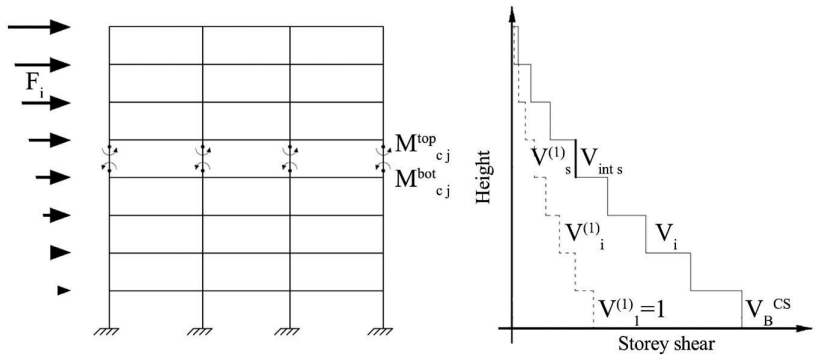


Figure 6. Assessment of the base shear capacity for a Column-Sway mechanism.

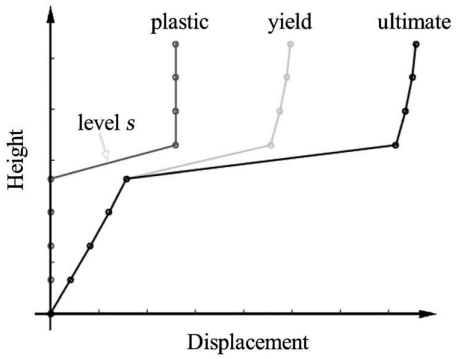


Figure 7. Displacement profile for a Column-Sway mechanism.

P-Delta effects might be added calculating the second-order OTM as per Sec. 2.3.1, dividing it by the effective height and subtracting this second-order base shear to the first-order base shear capacity.

$$F_i = \frac{m_i H_i}{\sum_i m_i H_i} V_B \tag{11}$$

$$V_i = \sum_i^n F_i \tag{12}$$

$$V_B^{CS} = \frac{V_{int\,s}}{V_s^{(1)}} \left(V_1^{(1)} = 1 \right) = \frac{V_{int\,s}}{V_s^{(1)}} \tag{13}$$

The yield drift at the soft-story level, θ_{sy}, is the minimum yield drift of the columns at that story. To calculate the drift demand at the other stories, the shear demand is divided by the secant-to-yielding stiffness of each story K^{CS} (Eq. 14, which indicates the shear force that produces a unit inter-story drift). The latter can be calculated using Eq. 15, in which i represents the considered story and j represents a column at that story.

$$\theta_i^y = \frac{V_i}{K_i^{CS}} \tag{14}$$

$$K_i^{CS} = \frac{\sum_j 12 E J_{sec,j}}{h_{int\,i}^2} \tag{15}$$

The "yielding" displacement profile Δ^y can be calculated recursively, starting from the drift of the first story. Once a soft story has developed, it is assumed that the plastic deformation concentrates only at level s. The plastic displacement profile Δ^p can be computed with Eq. 16, where θ_{su} is the minimum ultimate drift of the columns at level s. It is worth mentioning that two different columns can be responsible of the yield and ultimate drifts of level s. The yielding and plastic displacement are summed up to obtain the ultimate displacement profile Δ^u (Figure 7). Finally, the yield and ultimate displacement at the effective height are calculated with Eq. 8, while the effective height is calculated with Eq. 5.

$$\Delta_i^p = \begin{cases} 0 \text{ for } i < s \\ \left(\theta_s^u - \theta_s^y\right) h_{int\,s} \text{ for } i \geq s \end{cases} \quad (16)$$

It is worth mentioning that a linear force profile might not be adequate to represent the post-yielding behavior of a frame experiencing a soft-story mechanism. Therefore, it is generally suggested to repeat the abovementioned procedure by considering a uniform displacement profile (Eq. 17, where n is the number of stories) to verify such assumption.

$$F_i = \frac{1}{n} V_B \quad (17)$$

3. Numerical Investigation on a Set of Prototype Frame Structures

The SLaMA procedure, as originally proposed in NZSEE [2017] and in the refined version (without P-Delta effects), is herein applied to a set of case study frame structures. The nonlinear capacity curves and the related displacement profile are compared with the results of refined numerical pushover analyses. The accuracy of SLaMA is assessed in terms of the SLaMA-to-numerical error for some key parameters (i.e. displacement at the effective height at yielding and ultimate conditions, related effective height and ultimate base shear).
A set of 40 case study frames is used in this work (Fig. 8), including 2- or 4-bays frames with 2, 4, 6, 8 or 10 stories. These frames are intended to be the longitudinal frames of the buildings depicted in Fig. 8. It is worth mentioning that the assessment of the transverse frames is not considered in this paper. The contribution of the transverse frames (out-of- plane capacity) is neglected since it is significantly smaller than the in-plane capacity of the longitudinal ones. Internal columns, with negligible lateral load bearing capacity, are provided to resist gravity loads only. The layout of the structures is regular, with a bay length of 5.5 m and an inter-story height of 3.3 m. The database is divided into 4 subsets composed of 10 frames with 2 or 4 bays and 2, 4, 6, 8, 10 stories. Each subset is characterized by frames with different failure mechanism (i.e. Beam-Sway, Mixed-Sway, Column-Sway at the ground story, Column-Sway at mid height, see Sec. 3.2).

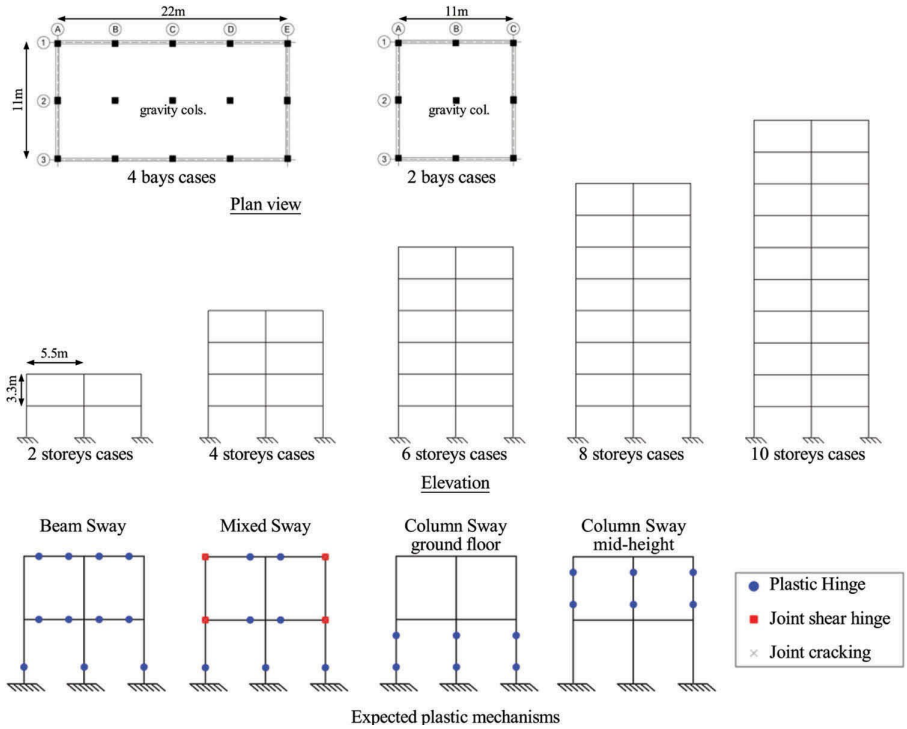


Figure 8. Case study matrix for the parametric analysis.

3.1 Materials Properties and Load Analysis

The material properties chosen for all the case studies are meant to be representative of the average values typical of existing RC structures [NZSEE, 2017, appendices C5E.1–C5E.3). A concrete compressive strength equal to f_0 25 MPa is used, since it is typical of RC buildings built in the 70s/80s. For the mechanical characterization of the structural members, concrete is modeled according to Mander *et al*. [1988], considering an elastic modulus equal to E_c¼5000 f_0. It is worth mentioning that 0.02 is conservatively considered as an upper bound for confined

c

concrete ultimate strain. The steel reinforcement of the beams is characterized by yield and ultimate stresses equal to f_y= 300 MPa and f_u= 390 MPa, respectively. A more resistant steel is used for the columns, with f_y= 450 MPa and f_u= 585 MPa, reflecting a common practice in existing buildings (e.g. in building #39 in; Pampanin *et al*., 2012]. In both cases, steel is modeled according to King *et al*. [1986], considering an elastic modulus E_s= 200 GPa and an ultimate strain ε_{su}= 0.06. The mean material properties are used in the mechanical characteriza- tion of the members for all the analyses.

The story seismic weight is constant along the height and it is approximately equal to 1035 and 2017 kN for the 2- and 4-bays buildings, respectively. This is done by consider- ing a concrete density equal to ρ_c = 25 kN/m^3, a superimposed dead load D_{sdl} = 0.5 kN/m^2 and a live load Q = 3 kN/m^2 reduced by a factor φ_e = 0.3 [NZS1170.5, 2004]. The axial load on the columns is calculated based on tributary areas.

3.2 Case Studies

3.2.1 Beam-Sway Subset (BS)

The frames of this group are designed according to Direct Displacement-Based Design [DDBD, Priestley *et al*., 2007] and capacity design provisions. Although no specific code/ standard is adopted for the design, the reinforcement details of the members (shown below) are compliant with the minimum design values for new structures [e.g. NZS 3101, 2006, NTC08, 2008]. They exhibit a global plastic mechanism in which, at ULS, all the beams have yielded, along with the base section of the ground story columns. DDBD approach is used imposing a design drift in the critical section, located at the ground story for frame structures, equal to 1.5% for 2- and 4-story cases and 1% for 6-, 8- and 10-story cases, as suggested in [Priestley *et al*., 2007]. The seismic demand is defined by a displacement response spectrum compliant with the New Zealand Code [NZS1170.5, 2004], related to a medium seismic intensity (peak ground acceleration, PGA = 0.25 g) and a shallow subsoil (corresponding to an average shear-wave velocity in the top 30 m of soil of $V_{s,30}$ = 360 m/s). It is worth noting that the design seismic intensity is not relevant for this study, since the main goal is to compare the nonlinear static capacity curves calculated with the SLaMA with the results of numerical pushover analyses.

Figure 9 summarizes the detailing of the adopted cross sections, along with the axial load ratios for columns. For both beams and columns, the transverse reinforcement ratio is equal to ρ_t = 0.75% in the plastic hinge zones. Five horizontal stirrups with 12 mm diameter and f_y= 450 MPa are provided in the joint panels, specifically designed to avoid shear failure (as confirmed in Sec. 4.2).

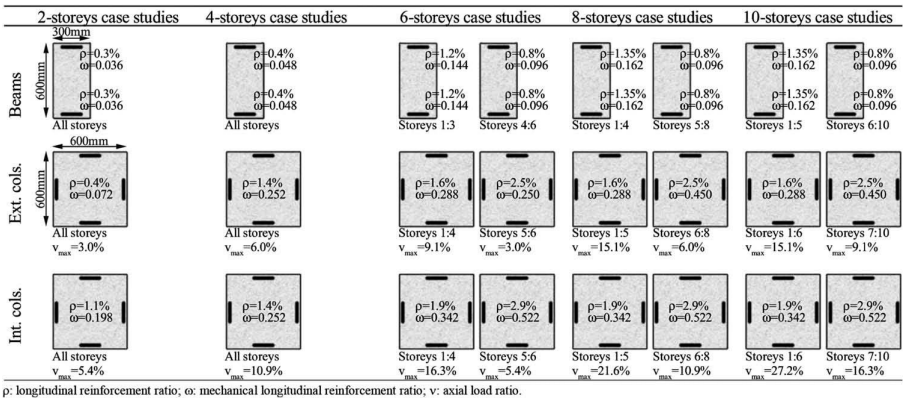


Figure 9. Beam-Sway subset: characteristics of beams and columns.

3.2.2 Mixed-Sway Subset (MS)

This group of structures is meant to represent buildings with a level of detailing typical of the 1970s (e.g. NZS1900, 1965), when capacity design principles were not yet introduced and the detailing of the joint shear reinforcement was not adequate to sustain seismic actions. In such conditions, shear cracking or shear failure of columns and joints might develop. The frames of this subset are obtained starting from the Beam-Sway subset, introducing structural weaknesses for the joints. In particular, no transverse reinforcement is considered in the joints and their principal tensile stress is limited to 0:3 f_c. The diameter of the transverse reinforcement of beams and columns is reduced and the spacing increased (ρ_t = 0.38%), in order to represent under-designed members typical of older RC structures [NZSEE, 2017]. The expected plastic mechanism for this subset of frames is characterized by a combination of beam and/or column plastic hinges and joint panels shear failure, called “shear hinge.”

3.2.3 Column-Sway, Soft Story at Ground Subset (CSg)

This subset represents pre-1970s frames designed for gravity loads only. The mechan- ical characteristics of the beams are equal to the Beam-Sway subset. The columns have a square cross-section with a 300 mm-side, and a reduced longitudinal reinfor- cement such that the flexural strength of the columns at the ground story is equal to 40% of the strength of the beams, thus allowing the undesirable "strong beam-weak column," typical of gravity-designed frames. Moreover, the transverse reinforcement ratio of the columns is reduced to $\rho_t = 0.2\%$, as observed in real pre-1970s buildings [Pampanin *et al*., 2012]. In this subset, rigid behavior is reasonably assumed for the joint panels, since the expected failure mechanism is a soft story locate at the ground story.

3.2.4 Column-Sway, Soft Story at Mid-Height Subset (CSmh)

This subset is meant to represent another typical situation for pre-1970s gravity- dominated frames: the reduction of the cross-section of the columns along the height due to the reduced gravity load. The mechanical characteristics of the beams are equal to the Beam-Sway subset. The columns have a 400 × 400 mm square cross-section, reducing to 300 × 300 mm at the building mid-height, where they have a flexural strength equal to 40% of the strength of the concurrent beams. Their transverse reinforcement ratio is $\rho_t = 0.2\%$. For these reasons, a soft-story mechanism is expected to develop at mid height of the building. As per the CSgf group, rigid behavior is assumed for the joint panels.

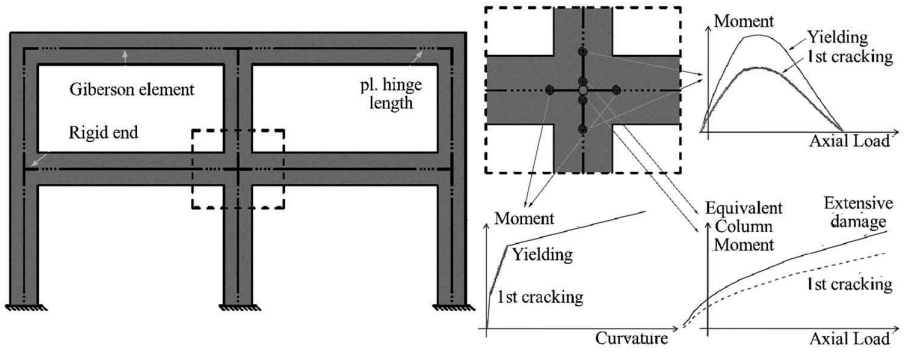


Figure 10. Numerical modeling strategy.

3.3 Numerical Modeling Assumptions

A numerical pushover analysis is performed for each frame using the software Ruaumoko [Carr, 2016]. The analyses are conducted in displacement-control and applying a linear force profile, consistently with the assumptions used in SLaMA. Since the aim of this work is the SLaMA versus numerical pushover validation only, the soft-story case studies are not re-assessed using a uniform force profile. P-Delta effects are neglected. This assump- tion is justified in Sec. 4. The analyses are terminated when the first member in the system reaches its ultimate displacement capacity. The floor slabs are modeled as rigid dia- phragms. Fully fixed boundary conditions are considered at the base of the columns.

The adopted modeling strategy (schematized in Fig. 10) was extensively validated against experimental tests both at subassembly and frame level [Magenes and Pampanin, 2004, Gentile *et al*., 2017a]. A lumped plasticity approach is adopted for beams and columns, which are modeled by means of mono-dimensional Giberson ele- ments [Sharpe, 1976]. The beams are characterized by means of trilinear Moment– Curvature relationships and plastic hinge length (see Sec. 2.1 for details) while for columns a Moment-Axial load domain is used to account for the variation of their capacity caused by the variation of axial load due to the frame Sway. Plastic hinge length ranges between 5.9% and 7.4% of the length for beams, and between 7.7% and 16.2% for columns. According to the state-of-the-art practice, hardening is considered for both beams and columns. Moment–Curvature analysis is performed using the software Cumbia [Montejo and Kowalsky, 2007] and the potential flange effect is accounted for with a 30% increase in the negative moment capacity. The ultimate drift of such members is calibrated consider- ing the alternative failure mechanisms as per Sec. 2.1 and Table 1. Rigid ends are used for beam and column members, which in turn are connected with nonlinear lumped springs (two for each geometrical node of the frame) used to model the joint panel. The nonlinear behavior of these springs is set consistently with the Equivalent Column Moment-joint drift relationships, depicted in Fig. 2.

4. Results

The accuracy of the SLaMA is assessed by comparing the results with the refined numerical pushover capacity curves an estimating thepercentage error

$(Err(\%) = \frac{SLaMA - P.O.}{P.O.})$

for a number of selected parameters.

First, the accuracy of the [NZSEE, 2017] version of the SLaMA procedure is assessed. Then, the improvements related to the use of the refined SLaMA are quantified. The synthetic description of the results allows to highlight the influence of the proposed refinements. Therefore, detailed results for the refined SLaMA are shown for selected cases, one for each subset, including the capacity curve, plastic mechanism and displacement profile.

The numerical curves are bilinearized by considering the stiffness secant to the first formed hinge in the system and calculating equivalent yield displacement applying the equal energy rule (as suggested in ATC 40, 1996 to estimate the effective period of the equivalent SDOF system and compare the capacity with the demand in the form of a response spectrum).

Table 2. Equivalent Column Moment for interior and exterior subassemblies.

Mechanism	Eq. Col. Moment (ext. sub-assembly)	Eq. Col. Moment (int. sub-assembly)
Column hinge (top or bottom)	M'_{cy}	M'_{cy}
Column Shear (top or bottom)	$l'_c V_c$	$l'_c V_c$
Beam hinge	$\frac{l'_c l_b}{l_c l'_b} M'_{by}$	$\frac{l'_c}{l_c}\left(\frac{l_{b,l}}{l'_{b,l}} + \frac{l_{b,r}}{l'_{b,r}}\right) M'_{by,l}$ (*) $\frac{l'_c}{l_c}\left(\frac{l_{b,l}}{l'_{b,l}} M'_{by,l} + \frac{l_{b,r}}{l'_{b,r}} M'_{by,r}\right)$ (**)
Beam Shear	$V_b l_b \frac{l'_c}{l_c}$	$V_b (l_{b,l} + l_{b,r}) \frac{l'_c}{l_c}$
Joint	$\frac{V_{jh} l'_c}{l_c \frac{l'_b}{l_b jd} - 1}$	$\frac{V_{jh} l'_c}{\frac{2l_c}{jd\left(\frac{l_{b,l}}{l'_{b,l}} \frac{l_{b,r}}{l'_{b,r}}\right)} - 1}$

where l_c is the distance between two contra-flexure points on the columns; $l_{0\,c}$ is the shear span of the column, $l_{b;l}$ is the distance between the joint centroid and the left beam mid-span, $l_{0\,b,l}$ is the shear span of the right beam, M^0_{cy} is the yield moment of the top (or bottom) column calculated at the joint interface, $M^0_{by;\,l}$ is the yield moment of the beam calculated at the joint interface, V_b is the beam shear capacity (left or right), V_c is the column shear capacity (top or bottom), V_{jh} is the joint shear capacity (at first cracking or failure), jd is the internal lever arm of the beam.
(*) It is assumed that only one beam yields. The right beam yielding moment should be used if $M_{by;\,r} < M_{by;l}$
(**) It is assumed that both beams yield.

Although a different bilinear fitting might give better estimation of the equivalent yield displacement [FEMA, 2009], this fitting method is adopted since it allows to define the hardening branch. The parameters selected for the comparison are the base shear, the effective height and the displacement at the effective height, calculated at yielding and ULS, and the secant-to-yielding stiffness. The effective height for the push- over analyses has been calculated with Eq. 5, based on the numerically calculated displacement profile. Moreover, the hierarchy of strength, the displacement profile and the full capacity curve are compared in a graphical fashion, for selected cases (one for each subset). Graphical results are available in Gentile [2017] for the complete set of case study frames.

It is worth stating that the main purpose of SLaMA is the assessment of existing structures. Hence, in most cases, the calculated capacity curve isuse to perform a capacity/demand check in the Acceleration-Displacement Response Spectrum (e.g. capacity spectrum method, ATC 40, 1996, or the percentage of building standard, NZSEE, 2017]. To this scope, the ultimate base shear and displacement are deemed to be the most relevant parameters.

4.1 Accuracy of SLaMA and Influence of the Proposed Refinements

In this section, the SLaMA-to-numerical percentage errors related to the [NZSEE, 2017] and the refined SLaMA procedures are compared. It is worth mentioning that since the [NZSEE, 2017] SLaMA procedure is not applicable for soft-story mechanisms located at mid height of the building, the comparison is only possible for the Beam-Sway, Mixed-Sway and Column-Sway ground story subsets. Figure 11 reports the comparison for each selected parameter: ultimate displacement (Fig. 14(a,b)), ultimate base shear (Fig. 14(c,d)), effective height (Fig. 14(a,e,f)), yield displacement (Fig. 14(a,g,h)) and initial stiffness (Fig. 14(a,i,j)). The capacity curves for the entire database, defined by means of the base shear and displacement at the significant points, are summarized in Table 3, both for the refined SLaMA and the numerical analyses.

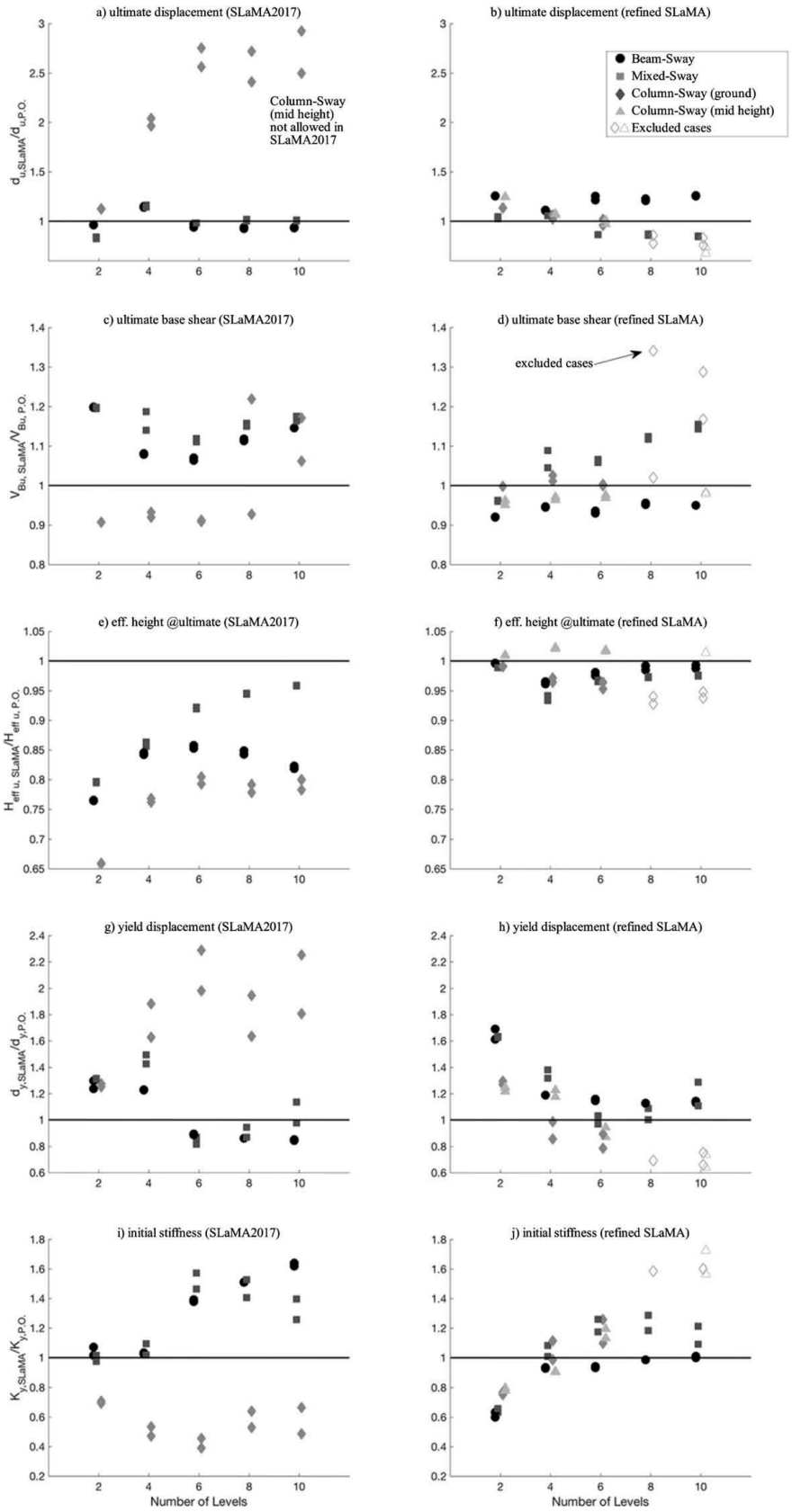


Figure 11. SLaMA-to-numerical error for both the [NZSEE, 2017] and refined SLaMA.

Table 3. Significant points of the numerical pushover curve for the entire database. The results for the refined SLaMA are reported in brackets.

Case Study	Δy [cm]			Δu [cm]		V_{By} [kN]		V_{Bu} [kN]	
BS	2b2s	1.17	(1.97)	13.41	(16.79)	382.3	(387.0)	420.8	(387.0)
	2b4s	2.55	(3.04)	23.85	(26.53)	485.2	(539.7)	570.1	(539.7)
	2b6s	5.71	(6.60)	43.89	(55.07)	848.3	(915.2)	978.2	(915.2)
	2b8s	7.60	(8.55)	59.01	(71.26)	836.6	(929.0)	971.7	(929.0)
	2b10s	9.28	(10.49)	69.89	(87.50)	795.3	(909.9)	958.2	(909.9)
	4b2s	1.23	(1.97)	13.37	(16.79)	772.7	(787.5)	855.6	(787.5)
	4b4s	2.55	(3.04)	24.03	(26.53)	915.9	(1009.2)	1068.0	(1009.2)
	4b6s	5.77	(6.60)	45.44	(55.07)	1649.1	(1779.0)	1913.0	(1779.0)
	4b8s	7.58	(8.55)	58.11	(71.26)	1629.7	(1814.4)	1906.0	(1814.4)
	4b10s	9.19	(10.49)	69.51	(87.50)	1560.2	(1781.7)	1876.0	(1781.7)
MS	2b2s	1.21	(1.98)	5.37	(5.50)	355.7	(366.7)	381.9	(366.7)
	2b4s	2.29	(3.02)	7.61	(8.18)	336.0	(479.9)	440.9	(479.9)
	2b6s	6.43	(6.64)	13.51	(11.65)	731.9	(887.0)	838.4	(887.0)
	2b8s	7.89	(8.59)	17.40	(15.13)	692.6	(893.7)	795.1	(893.7)
	2b10s	8.20	(10.54)	21.87	(18.62)	628.0	(881.2)	763.1	(881.2)
	4b2s	1.21	(1.98)	5.27	(5.50)	717.1	(766.8)	796.3	(766.8)
	4b4s	2.18	(3.02)	7.74	(8.18)	680.5	(948.4)	907.7	(948.4)
	4b6s	6.85	(6.64)	13.51	(11.65)	1433.3	(1749.8)	1642.0	(1749.8)
	4b8s	8.57	(8.59)	17.65	(15.13)	1379.3	(1778.5)	1592.0	(1778.5)
	4b10s	9.53	(10.54)	22.09	(18.62)	1305.8	(1753.3)	1534.0	(1753.3)
CSg	2b2s	1.89	(2.44)	3.55	(4.02)	76.8	(74.5)	74.6	(74.5)
	2b4s	2.30	(1.97)	2.39	(2.44)	101.0	(96.5)	94.1	(96.5)
	2b6s	2.42	(1.90)	2.84	(2.72)	208.0	(205.4)	204.8	(205.4)
	2b8s	3.29	(1.97)	3.50	(2.72)	320.4	(304.5)	298.5	(304.5)
	2b10s	2.67	(1.76)	3.01	(2.28)	215.4	(283.5)	220.1	(283.5)
	4b2s	1.92	(2.44)	3.54	(4.02)	138.9	(134.9)	135.2	(134.9)
	4b4s	1.99	(1.96)	2.29	(2.43)	160.1	(155.9)	154.1	(155.9)
	4b6s	2.09	(1.87)	2.64	(2.69)	335.0	(328.4)	328.6	(328.4)
	4b8s	2.76	(1.91)	3.11	(2.67)	360.0	(491.5)	366.6	(491.5)
	4b10s	2.14	(1.61)	2.57	(2.13)	341.6	(411.1)	352.1	(411.1)
CSmh	2b2s	1.83	(2.22)	6.53	(8.13)	126.5	(122.4)	128.7	(122.4)
	2b4s	2.03	(2.39)	3.83	(4.06)	119.4	(127.6)	132.5	(127.6)
	2b6s	2.79	(2.43)	5.11	(4.97)	273.1	(284.5)	293.9	(284.5)
	2b8s	2.97	(2.12)	4.38	(3.35)	279.4	(299.5)	307.8	(299.5)
	2b10s	3.89	(2.49)	5.14	(3.47)	301.7	(333.0)	340.1	(333.0)
	4b2s	1.77	(2.21)	6.54	(8.13)	222.7	(216.2)	224.7	(216.2)
	4b4s	1.95	(2.39)	3.78	(4.07)	207.5	(229.7)	236.6	(229.7)
	4b6s	2.58	(2.43)	4.93	(4.97)	470.1	(502.2)	514.8	(502.2)
	4b8s	2.72	(2.14)	4.19	(3.37)	495.0	(545.3)	557.4	(545.3)
	4b10s	3.40	(2.50)	4.72	(3.48)	517.4	(596.3)	606.9	(596.3)

BS: Beam-Sway; MS: Mixed-Sway; CSg: Column-Sway (ground); CSmh: Column-Sway (mid height); B: bays; s: – stories.

Figure 12 shows the pushover curves resulting from the numerical analyses. An in-depth discussion on the refined SLaMA results for each subset in the database is given in Sec. 3.2.1–3.2.4. It is worth mentioning that the numerical analyses have been repeated, by considering P-Delta effects, for the four tallest and widest case studies in the database. At the ultimate point, a maximum reduction in base shear with respect to the first-order analyses has been observed to be smaller than 10%, thus supporting the assumption of neglecting P-Delta effects.

For the Beam-Sway and Mixed-Sway subsets, the NZSEE2017 and the refined SLaMA procedures provide similar results and reasonable biases in terms of ultimate displacement (−20%, 20%). However, by using the proposed refinements, a substantial improvement in the estimation of the ultimate displacement is observed for frames exhibiting a Column-Sway mechanism at the ground story. Indeed, for such cases, the SLaMA 2017 procedure overestimates the ultimate displacement up to 200%, while for the refined SLaMA the mean error is below 20%. However, as discussed in Sec. 4.4, it is not recommended to use the refined SLaMA to calculate the Column-Sway capacity curve of frames with more than six stories.

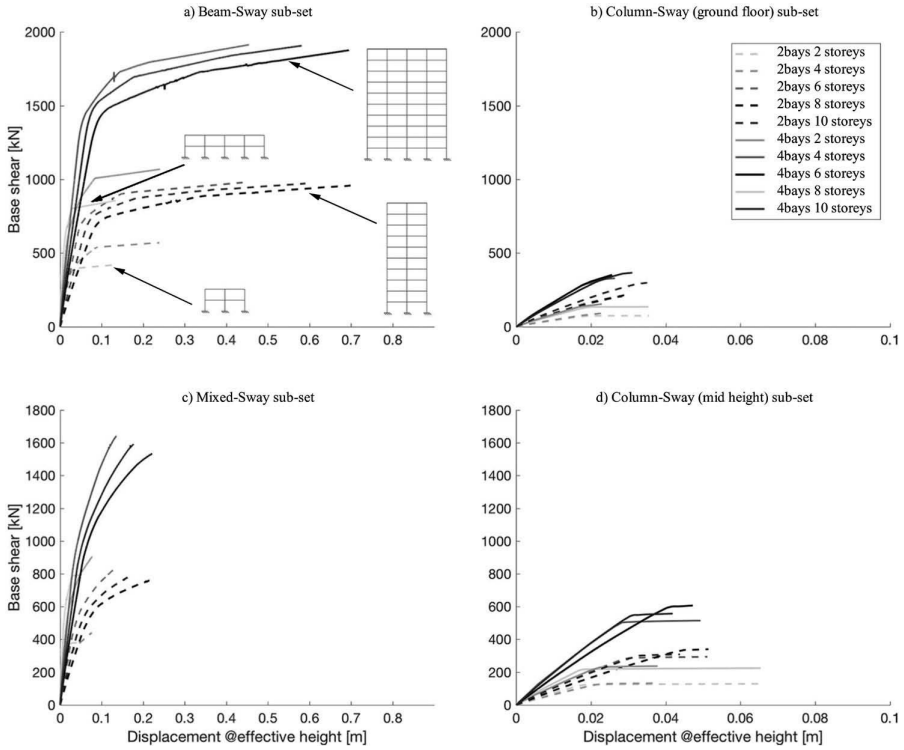


Figure 12. Numerical pushover capacity curves for the entire database.

In the refined procedure, the base shear at ULS is predicted with less than 10% error for the majority of the cases, compared to 20% average for the SLaMA 2017. It is deemed that such an improvement is due to the increased accuracy in the prediction of the effective height. Very simple formulations for the effective height are suggested in SLaMA 2017, leading to under predictions for this parameter up to 35%. On the other hand, the refined procedure allows to contain the error between 0.1% and 7.4%.

The refined SLaMA leads to a high dispersion (−30%, +75%) in the estimation of the yield displacement, and this is higher than the [NZSEE, 2017] procedure. Based on the observed error trends, further research is needed to improve the prediction of this parameter, especially at subassembly level. However, the observed error on the yield base shear (due to the elastic-perfectly plastic assumption in SLaMA) counterbalances the error on the yield displacement in the estimation of the initial stiffness. Regarding such a parameter, the refinements to the SLaMA procedure allow to narrow the error bandwidth, which ranges from (−60%, +60%) for SLaMA 2017 to (−40%, +20%) for the refined SLaMA.

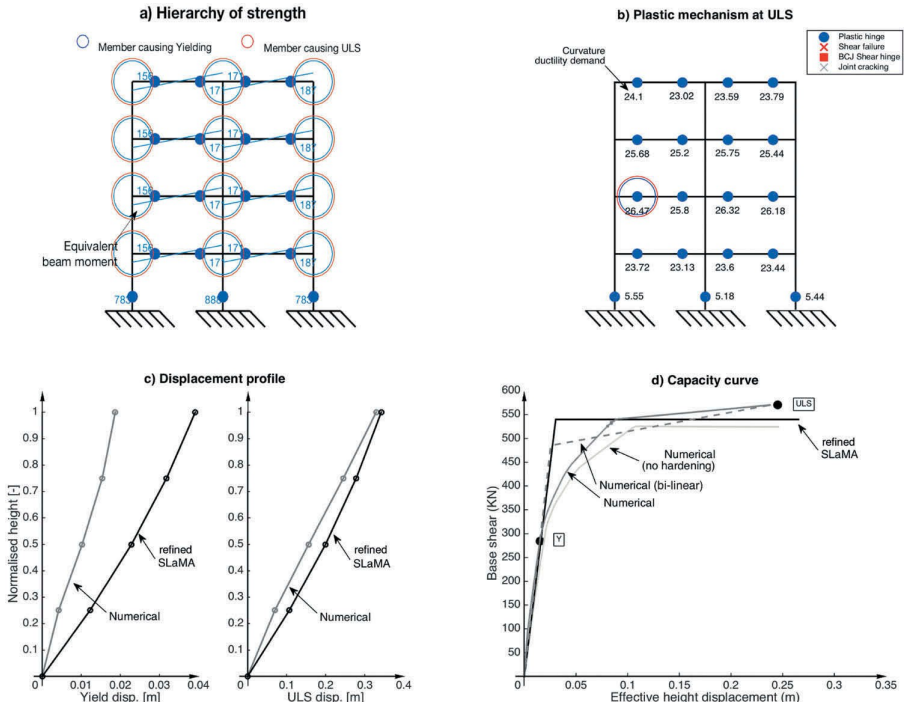


Figure 13. BS 2-bays, 4-stories: summary of the results.

Although the accuracy and reliability of the [NZSEE, 2017] version of the SLaMA is satisfactory, the proposed refinements are deemed to improve the construction of the capacity curve. As an improvement of the original procedure, the refinements allow to analyze frames with an expected soft-story mechanism at any level and also allow the calculation of the displacement profile for both global and local plastic mechanisms. A detailed analysis for the different subsets of the case study frames is reported in the following.

4.2 Beam-Sway Subset (BS)

For the studied Beam-Sway type frames, the ductility capacity of the beam that yields first (highlighted by a red circle in Fig. 13a,b) allows for a full redistribution of the internal actions, leading to a fully developed global mechanism. The hierarchy of strength is perfectly captured by SLaMA for all cases (compared in Fig. 13 with the pushover-based plastic mechanism). It is worth repeating that the proposed refinements to the SLaMA procedure are considered in this discussion. The same result is found for the effective height (maximum 1% error, see Table 4). This leads to underestimate the ultimate base shear (8%, on average), which is due to the hardening in the members, neglected in SLaMA. Figure 13d reports the results of the numerical pushover analysis carried out neglecting the hardening in the beam flexural strength. In this case, the error of the SLaMA procedure related to the ultimate base shear is zero, demonstrating the high accuracy of the procedure. The significant overestimation registered for the base shear at yielding (13% maximum) is due to assuming that all beams exploit the yielding moment demand at the yielding of the frame (which, in SLaMA, corresponds to the yielding of the first beam).

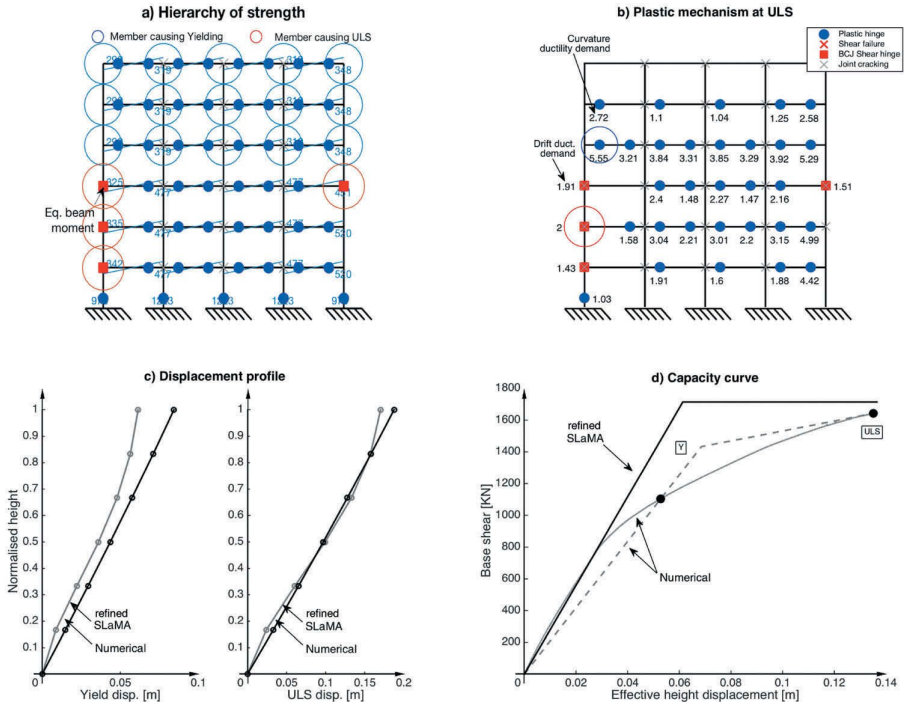


Figure 14. MS 4-bays, 6-stories: summary of the results.

This trend is consistent for all the case studies. Neglecting the strength hardening of the members approximately produces a 10% under-estimation of the base shear, as outlined in Fig. 13d. Indeed, neglecting hardening in SLaMA results in a slight and conservative underestimation of the peak strength.

The prediction of the displacement profile by using the refined SLaMA, both at yielding and ultimate, overestimates the numerical results (Fig. 13c). In particular, a 22% average error is registered for the yielding displacement at the effective height. On the other hand, the error on the ultimate displacement is approximately equal to 18%.

Table 4. BS subset SLaMA versus numerical [%].

CASE		Err($H_{eff,y}$)	Err($H_{eff,y}$)	Err(δ_y)	Err(δ_u)	Err(V_{By})	Err(V_{Bu})	Err(K_y)
2-bays	2-stories	−0.4	−0.3	68.9	25.2	1.2	−8.0	−40.8
	4-stories	−2.6	−3.9	18.9	11.2	11.2	−5.3	−15.9
	6-stories	−0.1	−0.4	7.0	16.0	5.7	−8.4	−13.6
	8-stories	−0.5	−0.1	7.0	14.8	9.4	−5.8	−11.1
	10-stories	−1.2	−0.5	10.2	22.0	13.5	−5.8	−11.6
4-bays	2-stories	−0.2	−0.4	61.1	25.6	1.9	−8.0	−37.9
	4-stories	−2.1	−3.5	18.8	10.4	10.2	−5.5	−15.8
	6-stories	0.3	0.1	5.9	12.0	5.7	−8.9	−12.7
	8-stories	0.0	0.7	7.2	16.6	9.7	−6.2	−11.3
	10-stories	−0.7	0.1	11.4	22.7	13.3	−5.7	−12.5
Mean error		−0.8	−0.8	21.6	17.7	8.2	−6.8	−18.3

4.3 Mixed-Sway Subset (MS)

In the case study frames of this subset, the ultimate displacement capacity of the structure is governed by the beam-column joint that first reaches its ultimate deformation capacity (highlighted in a red circle in Fig. 14). This strongly affects the possibility to redistribute the internal actions and hence the formation of a global plastic mechanism. Among the analyzed case studies, full redistribution is only achieved for frames up to four stories. For example, Fig. 13 shows the results of the refined SLaMA for the 6-stories frame, which does not develop a full mechanism. The assumption, in SLaMA, of calculating the ultimate base shear assuming the development of the full strength of all the sub-assemblies results in an overestimation. This error monotonically increases with the number of stories (maximum 15%, see Table 5 and Fig. 14d). For the same reason discussed in Sec. 4.1, a higher overestimation of the base shear at yielding is registered (25% on average).

The ultimate displacement profile and, in turn, the ultimate displacement at the effective height, is reasonably well-predicted for frames developing a Mixed-Sway mechan- ism. In particular, for the cases in which the frame ULS is governed by the failure of a joint panel, the ultimate displacement is slightly overestimated (about 3%). A good match can be observed for the yield displacement of the 6-, 8-, 10-stories frames, while a great over-estimation arises for the 2- and 4-stories cases.

Finally, similarly to the results observed for the Beam-Sway subset (Sec. 4.1), the effective height shows an almost perfect match between SLaMA and numerical pushover. This con- firms that the assumed displacement shapes in the refined SLaMA procedure are appropriate.

4.4 Column-Sway Subsets: Ground (CSg) and Mid-Height (CSmh)

Similar results can be observed applying the refined SLaMA to the two subsets of frames experiencing a soft-story mechanism. Hence, the related results are presented together. For all the case study frames, the hierarchy of strength calculations allow to accurately predict the location of the soft story (see, for example, Figs. 15(a,b) and 16(a,b)). Thus, it can be generalized that the proposed procedure for Column-Sway mechanisms can be used to detect the location of a soft-story mechanism which may develop at any story.

Table 5. MS subset SLaMA versus numerical error [%].

CASE		Err($H_{eff,y}$)	Err($H_{eff,y}$)	Err(δ_y)	Err(δ_u)	Err(V_{By})	Err(V_{Bu})	Err(K_y)
2-bays	2-stories	−0.7	−1.0	63.4	2.5	3.1	−4.0	−38.8
	4-stories	−3.5	−6.7	31.8	7.5	42.8	8.8	−24.1
	6-stories	−0.2	−1.5	−4.6	1.0	18.7	3.6	−3.1
	8-stories	−0.4	−1.4	3.5	−2.7	27.2	10.8	−8.2
	10-stories	−1.2	−1.8	25.3	−9.7	39.3	14.6	−22.2
4-bays	2-stories	−0.4	−1.1	62.8	4.4	6.9	−3.7	−38.6
	4-stories	−2.6	−5.8	38.1	5.7	39.4	4.5	−27.6
	6-stories	0.1	−1.2	−10.5	1.0	19.6	4.4	3.3
	8-stories	0.0	−1.2	−4.7	−4.1	27.1	10.1	−0.2
	10-stories	−0.6	−1.6	7.9	−10.6	33.2	13.4	−9.7
Mean error		−1.0	−2.3	21.3	−0.5	25.7	6.3	−16.9

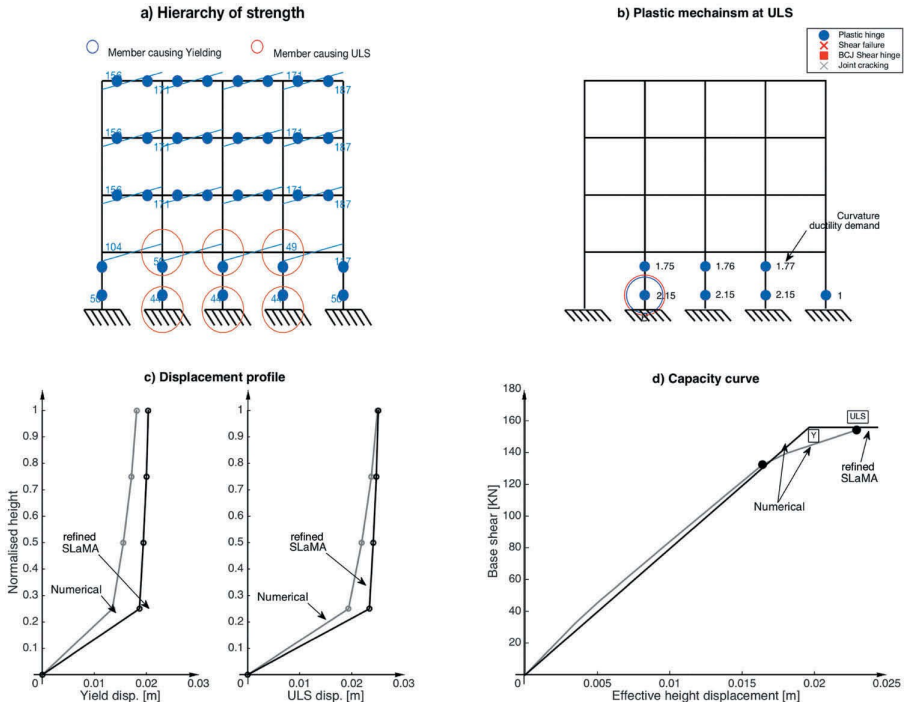


Figure 15. CSgf 4-bays, 4-stories: summary of the results.

The proposed SLaMA procedure is able to predict the base shear capacity of the frame very accurately (Tables 6 and 7 indicate less than 5% average over estimation on the yield and ultimate base shear). However, SLaMA greatly overestimates the base shear capacity for tall frames, for which full development of the soft story is prevented by the drift capacity of the first formed hinge. This happened for the 10-story cases with a ground soft-story (see Table 6).

The effective height, which is not expressly used in the SLaMA calculations for a Column-Sway mechanism, is calculated with great accuracy both at yielding and ultimate (4% error, in average). This reflects the match between the assumed (SLaMA) and the "actual" (numerical pushover) displacement profiles (see Figs. 15c and 16c) also for the Column-Sway frames.

The SLaMA procedure is able to accurately predict both the yield and ultimate displacements for frames with 2, 4 and 6 stories. Conversely, for the 8- and 10-stories frames there is a great under estimation of these parameters (higher than 20%, see Tables 6 and 7) and this greatly affects the SLaMA capacity curve. This gap is caused by an error in assessing the contribution to the total displacement of the stories not involved in the soft story. Since this major error is registered for both the CSg and CSmh subsets, it is not recommended to use SLaMA to calculate the Column-Sway capacity curve of frames having more than six stories. For this reason, the average values of the error in Tables 6 and 7 are referred to the frames with 2, 4 and 6 stories. Finally, Figs. 15d and 16d should be compared to assess the different accuracy of SLaMA for short and tall Column-Sway type frames.

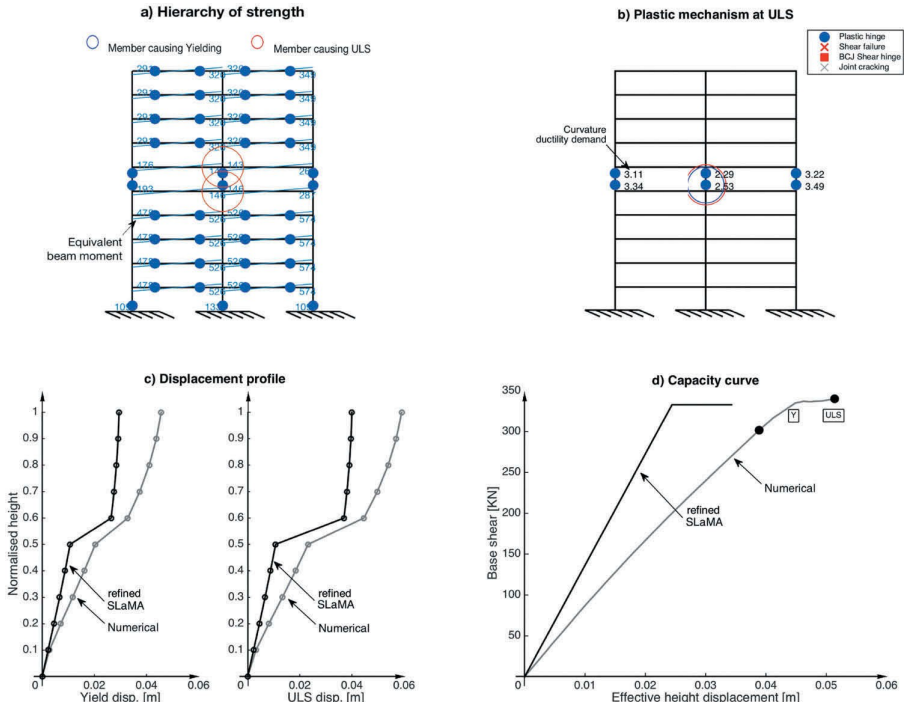


Figure 16. CSmh 2-bays, 10-stories: summary of the results.

Table 6. CSgf-Sway subset SLaMA versus numerical error [%].

CASE		Err($H_{eff,y}$)	Err($H_{eff,y}$)	Err(δ_y)	Err(δ_u)	Err(V_{By})	Err(V_{Bu})	Err(K_y)
2-bays	2-stories	−1.7	−0.9	29.7	13.5	−3.0	−0.2	−22.7
	4-stories	−3.7	−3.6	−14.3	2.3	−4.5	2.6	16.7
	6-stories	−4.6	−4.7	−21.6	−4.2	−1.2	0.3	27.4
	8-stories	−6.5	−7.4	−40.4	−22.6	−5.0	2.0	66.8
	10-stories	−4.9	−6.3	−34.7	−24.8	31.6	28.8	51.7
4-bays	2-stories	−1.5	−0.8	27.2	13.7	−2.9	−0.2	−21.2
	4-stories	−3.2	−2.8	−1.1	6.3	−2.6	1.1	1.2
	6-stories	−4.0	−3.6	−10.6	2.0	−2.0	−0.1	12.0
	8-stories	−5.8	−6.0	−30.6	−14.0	−5.9	0.6	44.4
	10-stories	−4.6	−5.2	−24.8	−17.0	20.4	16.8	33.1
Mean error		−3.1	−2.7	1.6	5.6	−2.7	0.6	

Table 7. CSmh subset SLaMA versus numerical error [%].

CASE		Err($H_{eff,y}$)	Err($H_{eff,y}$)	Err(δ_y)	Err(δ_u)	Err(V_{By})	Err(V_{Bu})	Err(K_y)
2-bays	2-stories	3.2	1.0	21.5	24.5	−3.3	−4.9	−17.7
	4-stories	4.0	2.5	3.6	6.0	−5.8	−3.7	−15.0
	6-stories	2.4	2.2	−23.3	−3.0	−7.5	−3.2	14.8
	8-stories	1.2	2.1	−41.8	−24.2	−11.0	−2.7	40.6
	10-stories	0.6	1.9	−53.2	−33.3	−17.7	−2.1	56.3
4-bays	2-stories	3.0	0.9	24.7	24.3	−2.9	−3.8	−19.8
	4-stories	3.6	2.3	4.9	7.5	−5.3	−2.9	−18.5
	6-stories	2.1	1.9	−17.9	0.7	−6.5	−2.4	6.1
	8-stories	1.0	1.8	−35.5	−19.9	−8.8	−2.2	27.3
	10-stories	0.6	1.8	−45.8	−26.7	−14.2	−1.7	35.8
Mean error		3.1	1.8	2.3	10.0	−5.2	−3.5	10.9

5. Final Remarks

This work deals with the seismic assessment of the nonlinear capacity of RC bare frames through the SLaMA. The original analytical procedure proposed in the NZSEE [2017] seismic assessment guidelines is herein discussed and extensively validated through nonlinear pushover analyses on fra systems, b considering potential areas of improvement or extension to be of immediate and practical use for the reader/user of the NZSEE guidelines. A revised procedure for RC frames is proposed and numerically validated.

It is worth noting that this paper, developed during the preparation of the guideline document itself and further refined after its publication, represents the first extensive validation of the SLaMA 2017 version available in literature and thus can be used as a scientific background document. However, further research is needed to extend SLaMA to include infill-frame interaction and systematically validate the procedure on 3D, tor- sion-prone buildings.

Both the original and the refined SLaMA procedures are applied to 40 case study frames with different geometry (2, 4, 6, 8 or 10 stories, 2 or 4 bays) and expected plastic mechanisms. The database included "Beam-Sway" frames, typical of more recent "capa- city-designed" structures, "Column-Sway" frames, with a local soft-story mechanism (either at ground or at mid-height), and "Mixed-Sway" frames, typical of under- designed structures with lack of capacity design provisions and poorly detailed joint panels susceptible to shear failure. The resulting force–displacement capacity curves are compared to refined numerical pushover analyses in order to assess the accuracy and the reliability of the SLaMA [NZSEE, 2017] and the proposed refined SLaMA. The main findings can be summarized as follows:

- The SLaMA 2017 procedure is overall proved to be an accurate and reliable tool for the seismic performance assessment of RC frames with different failure mechanisms. A set of ad-hoc equations is herein proposed for RC frames exhibiting a soft-story mechanisms involving higher-than ground level stories, for which the original pro-cedure does not provide an explicit solution. Moreover, a systematic error is observed in the estimation of the effective height for different plastic mechanisms. The proposed refinements to the procedure allow to overcome the above-mentioned gaps and to calculate the displacement profile of the frame;
- With reference to Beam-Sway and Mixed-Sway subsets, the NZSEE2017 and the refined SLaMA procedures provide similar results and reasonable biases in terms of ultimate displacement (−20%, 20%). On the other hand, the proposed refinements allow to considerably reduce the error for frames exhibiting a Column-Sway mechan-ism at the ground story;
- In the refined procedure, the base shear at ULS is predicted with less than 10% error for the majority of the cases, compared to 20% average for the SLaMA 2017. It is deemed that such an improvement is due to the increased accuracy in the prediction of the effective height, with errors ranging between the 0.1% and 7.4%;
- The refined SLaMA still shows a relatively high dispersion [−30%, +75%] in the estimation of the yield displacement. Based on the observed error trends, further research is needed to improve the prediction of this parameter, especially at subassem- bly level. Nevertheless, the observed error on the yield base shear (due to the adopted elastic-perfectly plastic assumption in SLaMA) counterbalances the error on the yield displacement in the estimation of the initial stiffness. Regarding such a parameter, the refinements to the SLaMA procedure allow to narrow the error bandwidth, which goes from [−60%, +60%] for SLaMA 2017 to [−40%, +20%] for the refined SLaMA.

Based on the results of this work, it is deemed that the refined SLaMA procedure is a reliable method for the seismic assessment of frames with a maximum of 10 stories, which restricts to 6 stories if a Column-Sway mechanism is predicted.

6. Acknowledgements

This study was performed in the framework of the "SAFER Concrete Technology" and "Advancements in Engineering Guidelines and Standards" projects, funded by the New Zealand Natural Hazard Research Platform (NHRP) and of the PE 2014–2018 joint program DPC (Italian Department of Civil Protection) - ReLUIS (Laboratories University Network of Seismic Engineering).

7. Funding

This study was performed in the framework of the "SAFER Concrete Technology" and "Advancements in Engineering Guidelines and Standards" projects, funded by the New Zealand Natural Hazard Research Platform (NHRP) and of the PE 2014–2018 joint program DPC (Italian Department of Civil Protection) - ReLUIS (Laboratories University Network of Seismic Engineering).

8. ORCID

Roberto Gentile http://orcid.org/0000-0002-7682-4490
Ciro del Vecchio http://orcid.org/0000-0002-4912-2944
Stefano Pampanin http://orcid.org/0000-0002-2714-6697

9. References

ATC 40. [1996] *Seismic evaluation and retrofit of concrete buildings, Applied Technology Council*, Redwood City, California, USA.

Berry, M. P. and Eberhard, M. O. [2005] "Practical performance model for bar buckling," *Journal of Structural Engineering*, 131, 1060–1070. doi:10.1061/(ASCE)0733-9445(2005)131:7(1060).

Borzi, B., Pinho, R. and Crowley, H. [2008] "Simplified pushover-based vulnerability analysis for large-scale assessment of RC buildings," *Engineering Structures*, 30, 804–820. doi:10.1016/j. engstruct.2007.05.021.

Calvi, G. M., Magenes, G. and Pampanin, S. [2002] "Relevance of beam-column joint damage and collapse in RC frame assessment," *Journal of Earthquake Engineering*, 6(1), 75–100. doi:10.1080/ 13632460209350433.

Cardone, D. and Flora, A. [2017] "Multiple inelastic mechanisms analysis (MIMA): A simplified method for the estimation of the seismic response of RC frame buildings," *Engineering Structures*, 145(15), 368–380. doi:10.1016/j.engstruct.2017.05.026.

Carr, A. J. [2016]. "*RUAUMOKO2D* - The Maori god of volcanoes and earthquakes," Inelastic Analysis Finite Element program, Christchurch, New Zealand.

Crowley, H., Pinho, R. and Bommer, J. [2004] "A probabilistic displacement-based vulnerability assessment procedure for earthquake loss estimation," *Bulletin of Earthquake Engineering*, 2(2), 173–219. doi:10.1007/s10518-004-2290-8.

Del Vecchio, C., Del Zoppo, M., Di Ludovico, M., Verderame, G. M. and Prota, A. [2017c] "Comparison of available shear strength models for non-conforming reinforced concrete columns," *Engineering Structures*, 148, 312–327. doi:10.1016/j.engstruct.2017.06.045.

Del Vecchio, C., Di Ludovico, M., Balsamo, A. and Prota, A. [2018a] "Seismic retrofit of real beam-column joints using fiber reinforced cement (FRC) composites," *ASCE Journal of Structural Engineering*, 144(5). doi:10.1061/(ASCE)ST.1943-541X.0001999

Del Vecchio, C, Di Ludovico, M, Pampanin, S, and Prota, A. [2018] "Repair costs of existing RC buildings damaged by the L'aquila earthquake and comparison with FEMA P-58 predictions," *Earthquake Spectra*, 34, 237–263.

Del Vecchio, C., Gentile, R., Di Ludovico, M., Uva, G. and Pampanin, S. [2018b] "Implementation and validation of the Simple Lateral Mechanism Analysis (SLaMA) for the seismic performance assessment of a damaged case study building," *Journal of Earthquake Engineering*, in press. 1–32. doi:10.1080/13632469.2018.1483278

Del Vecchio, C., Gentile, R. and Pampanin, S. [2017a]. "*The Simple Lateral Mechanism Analysis (SLaMA) for the seismic performance assessment of a case study building damaged in the 2011 Christchurch earthquake*," Research report N. 2016-02, University of Canterbury, Christchurch, New Zealand.

Elwood, K. J. and Moehle, J. P. [2005] "Axial capacity model for shear-damaged columns," *ACI Structural Journal*, 102(4), 578–587.

FEMA. [2009] *Quantification of Building Seismic Performance Factors, FEMA P695*, Federal Emergency Management Agency, Washington D.C., USA, pp. 421.

Gentile, R. [2017]. "Extension, refinement and validation of the Simple Lateral Mechanism Analysis (SLaMA) for the seismic assessment of RC structures," PhD thesis, Department of Civil, Environmental and Landscape, Building Engineering and Chemistry, Polytechnic University of Bari, Bari, Italy.

Gentile, R., Del Vecchio, C. and Pampanin, S. [2017a]. "Seismic assessment of a RC case study building using the Simple Lateral Mechanism Analysis, SLaMA, method," *6th ECCOMAS Thematic Conference on Computational Methods in Structural Dynamics and Earthquake Engineering*, Rhodes Island, Greece, 15–17 June 2017.

Gentile, R., Fondi, L. and Pampanin, S. [2017b]. "Vulnerabilità sismica di classi di edifici a telaio in C.A.: sensibilità della probabilità di superamento dello SLV ai dettagli costruttivi e ai materiali adottati (in Italian)," *XVII Convegno 'L'ingegneria Sismica in Italia' (ANIDIS)*, Pistoia, Italy.

King, D. J., Priestley, M. J. N. and Park, R. [1986]. "Computer programs for concrete column design, Research Report 86/12," Department of Civil Engineering.

Kowalsky, M. J. and Priestley, M. J. N. [2000] "Improved analytical model for shear strength of circular reinforced concrete columns in seismic regions," ACI Structural Journal, 97, 388–396.

Magenes, G. and Pampanin, S. [2004]. "Seismic response of gravity-load design frames with masonry infills," *13th World Conference on Earthquake Engineering*, Vancouver, British Columbia, Canada.

Mander, J. B., Priestley, M. J. N. and Park, R. [1988] "Theoretical stress strain model for confined concrete," *Journal of Structural Engineering*, 114(8), 1804–1826. doi:10.1061/(ASCE)0733-9445- (1988)114:8(1804).

Montejo, L. A. and Kowalsky, M. J. [2007] *Set of Codes for the Analysis of Reinforced Concrete Members*, North Carolina State University, Raleigh, North Carolina.

NTC08. [2008]. "DM 14 gennaio 2008 in materia di 'norme tecniche per le costruzioni'," Gazzetta ufficiale n.29 del 4 febbraio 2008, Ministero delle Infrastrutture e dei trasporti, istituto Poligrafico e Zecca dello stato. Rome, Italy.

NZS 1900, 1965. "Model building bylaw: Basic design loads and commentary," NZS 1900. Standards Association of New Zealand, Wellington, NZ.

NZS 1900.8:1965. "Model building bylaw: Basic design loads and commentary," NZS 1900. Standards Association of New Zealand, Wellington, NZ.

NZS1170.5. [2004] Structural Design Actions, Standards New Zealand, Wellington, New Zealand. NZS3101. [2006] Part 1: Concrete Structures Standard - The Design of Concrete Structures, Standards

New Zealand, Wellington, New Zealand.

NZSEE. [2006] New Zealand Society for Earthquake Engineering, Assessment and Improvement of the Structural Performance of Buildings in Earthquakes, New Zealand Society for Earthquake Engineering, Wellington, New Zealand.

NZSEE. [2017] New Zealand Society for Earthquake Engineering, the Seismic Assessment of Existing Buildings - Technical Guidelines for Engineering Assessments, New Zealand Society for Earthquake Engineering, Wellington, New Zealand.

Pampanin, S., Bolognini, D. and Pavese, A. [2007] “Performance-based seismic retrofit strategy for existing reinforced concrete frame systems using fiber-reinforced polymer composites,” Journal of Composites for Construction, 11(2), 211–226. doi:10.1061/(ASCE)1090-0268(2007)11:2(211).

Pampanin, S., Calvi, G. M. and Moratti, M. [2002]. “Seismic behaviour of RC beam-column joints designed for gravity loads,” 12th European Conference on Earthquake Engineering, London, UK. Pampanin, S., Kam, W. Y., Akguzel, U., Tasligedik, A. S. and Quintana Gallo, P. [2012] Seismic Performance of Reinforced Concrete Buildings in the Christchurch CBD in 22 February 2011

Earthquake Part I: Overview, University of Canterbury, Christchurch, New Zealand.

Pampanin, S., Magenes, G. and Carr, A. [2003]. “Modelling of shear hinge mechanism in poorly detailed RC beam-column joints,” fib Symposium 2003: “Concrete Structures in Seismic Regions”, Athens, Greece.

Priestley, M. [1997] “Displacement-based seismic assessment of reinforced concrete buildings,”

Journal of Earthquake Engineering, 1(1), 157–192. doi:10.1080/13632469708962365.

Priestley, M. and Calvi, G. [1991] “Towards a capacity-design assessment procedure for reinforced concrete frames,” Earthquake *Spectra*, 7(3), 413–437. doi:10.1193/1.1585635.

Priestley, M., Seible, F. and Calvi, G. M. [1996] *Seismic Design and Retrofit of Bridges*, John Wiley and Sons, New York, USA.

Priestley, M. J. N., Calvi, G. M. and Kowalsky, M. J. [2007] *Displacement-Based Seismic Design of Structures*, IUSS Press, Pavia, Italy.

Quintana Gallo, P. [2014]. “The nonlinear dynamics involved in the seismic assessment and retrofit of reinforcement concrete buildings,” PhD thesis, Department of Civil and Natural Resource Engineering, University of Canterbury.

Sharpe, R. D. [1976]. “The Seismic Response of Inelastic Structures,” PhD thesis, Department of Civil Engineering, University of Canterbury, Christchurch, New Zealand.